



Synthesis and photocatalytic properties of tetragonal tungsten bronze type oxynitrides

Katsuya Shimizu, Hideki Kato*, Makoto Kobayashi, Masato Kakihana

Institute of Multidisciplinary Research for Advanced Materials, Tohoku University, 2-1-1 Katahira, Aoba-ku, Sendai, Miyagi 980-8577, Japan

ARTICLE INFO

Article history:

Received 28 December 2016

Received in revised form 16 January 2017

Accepted 22 January 2017

Available online 23 January 2017

Keywords:

Hydrogen evolution

Visible-light-driven photocatalyst

Tetragonal tungsten bronze

ABSTRACT

Synthesis of a series of oxynitride $\text{Ba}_{3-x}\text{La}_x\text{Ta}_5\text{O}_{14-x}\text{N}_{1+x}$ ($x=0-1.5$) with a tetragonal tungsten bronze (TTB) structure was examined using moist- NH_3 and 5% $\text{NH}_3\text{-N}_2$ as nitriding atmosphere. The samples with $x=0-1$ were successfully obtained as phase pure TTB oxynitride whereas the $x=1.5$ samples gave a mixture of TTB oxynitride, Ta_3N_5 , and LaTaO_4 . Absorption of TTB oxynitrides in visible region was enhanced as increasing the content of nitrogen. TTB oxynitrides exhibited both of H_2 and O_2 evolution under visible light in the presence of methanol and silver ions, respectively, as sacrificial reagents. Nitrogen poor surface in the samples synthesized under moist- NH_3 atmosphere was modified by annealing treatment using 5% NH_3 , resulting in improvement of photocatalytic activity for H_2 evolution. Evaluation using monochromatic light revealed that the apparent quantum efficiency of $\text{Ba}_2\text{LaTa}_5\text{O}_{13}\text{N}_2$ was higher than that of $\text{Ba}_3\text{Ta}_5\text{O}_{14}\text{N}$.

© 2017 Elsevier B.V. All rights reserved.

1. Introduction

Water splitting photocatalysts have attracted much attention as a potential method for the solar hydrogen production [1–5]. Various kinds of research, such as development of new photocatalysts [6–23], cocatalysts [17,24–30], synthesis method [31–38], and modification [39–43], are conducted to make progress in photocatalytic water splitting. Crystal structure is an important factor to classify photocatalyst materials. Perovskite structure is known as a promising one for photocatalysts in both of oxide and oxynitride [1–3,10,12,13,21,41]. $\text{SrTiO}_3\text{:Al}$ and $\text{NaTaO}_3\text{:La}$, representative perovskite-type oxide photocatalysts, can split water with very high quantum efficiency [44,45]. These photocatalysts function under only ultraviolet excitation whereas many perovskite-type photocatalysts with response to visible light are also reported. $\text{SrTiO}_3\text{:Rh}$ is a well known visible light responsive oxide photocatalyst for H_2 evolution [32,39,43,46]. In the oxynitride system, many perovskite-type ABO_2N , ABON_2 , and solid solutions are reported as visible light responsive photocatalysts and photoanodes [1–3,12,13,17,21,31,34,36,40,41]. Especially, Domen and co-workers have recently achieved overall water splitting under visible light using $\text{LaMg}_{1/3}\text{Ta}_{2/3}\text{O}_2\text{N}$ modified with a metal oxyhydroxide layer [41]. In perovskite structure, MX_6 octahe-

dra share corners with other octahedra to built characteristic framework. Tetragonal tungsten bronze (TTB) structure is common structure for materials with a general formula $(\text{A}1)(\text{A}2)_2\text{B}_5\text{X}_{15}$ and is regarded as perovskite-related structure because it is also constituted of framework with corner-shared MX_6 octahedra like as the perovskite structure (Fig. 1). Many TTB compounds, such as $\text{K}_2\text{Ln}(\text{Nb},\text{Ta})_5\text{O}_{15}$ (Ln = lanthanide), $\text{KM}_2\text{Nb}_5\text{O}_{15}$, and tetr-BaTa₂O₆, can drive overall water splitting and/or CO_2 reduction in water under ultraviolet irradiation [1–3,11,37]. Nitride and oxynitride are attractive material group for visible-light-driven photocatalysts because N 2p orbital form valence band at shallower position than O 2p orbital [47]. Most of oxynitride photocatalysts are of perovskite compounds especially for d⁰-based oxynitrides whereas oxynitrides with other structures such as TaON , GaN:ZnO , C_3N_4 , $\text{Y}_2\text{Ta}_2\text{O}_5\text{N}$ and $\text{MgTa}_2\text{O}_{6-x}\text{N}_y$ are also reported [1–3,6,19]. Lerch et al. have recently succeeded in synthesis of a TTB oxynitride $\text{Ba}_3\text{Ta}_5\text{O}_{14}\text{N}$ using a mixed gas of NH_3 and O_2 and revealed that $\text{Ba}_3\text{Ta}_5\text{O}_{14}\text{N}$ modified with a cocatalyst is active for H_2 evolution from an aqueous methanol solution under visible light [22]. Here we report synthesis of nitrogen content-controlled $\text{Ba}_{3-x}\text{La}_x\text{Ta}_5\text{O}_{14-x}\text{N}_{1+x}$ using either moist- NH_3 or $\text{NH}_3\text{-N}_2$ atmosphere. Effects of annealing treatment on properties of surfaces and photocatalytic activities are also discussed.

* Corresponding author.

E-mail address: hkato@tagen.tohoku.ac.jp (H. Kato).

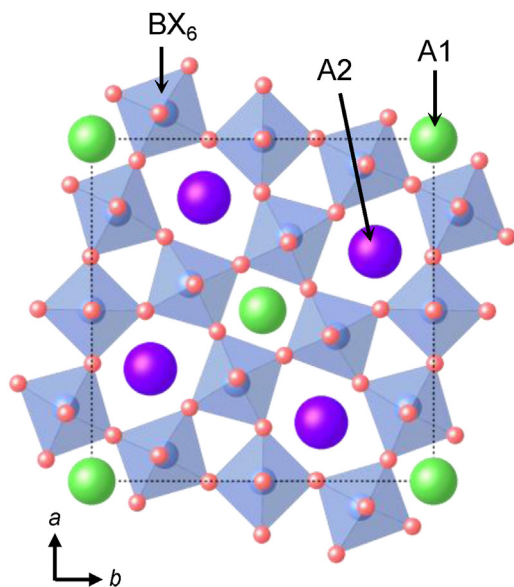


Fig. 1. General crystal structure of TTB compound $(A_1)(A_2)_2B_5X_{15}$.

2. Experimental

2.1. Synthesis of $Ba_{3-x}La_xTa_5O_{14-x}N_{1+x}$

Powders of TTB-type oxynitrides $Ba_{3-x}La_xTa_5O_{14-x}N_{1+x}$ were synthesized by nitridation of the corresponding amorphous oxide precursors. The precursors were obtained by a polymerizable complex method employing citric acid (CA, Wako Pure Chemical, 98%) and propylene glycol (PG, Kanto Chemical, 99.0%) as described elsewhere [21]. Barium carbonate (Kanto Chemical, 99.9%), lanthanum nitrate hexahydrate (Wako Pure Chemical, 99.9%), tantalum chloride (Furuuchi Chemical, 99.9%) were used as raw materials. PG, $BaCO_3$, and $La(NO_3)_3 \cdot 6H_2O$ were added to a methanol solution dissolving $TaCl_5$. The solution was heated at 353 K with stirring until being a transparent solution and was heated at 423 K to promote condensation and esterification between CA and PG. The obtained viscous resin matter was subjected to sequential heating at 523, 623, and 723 K using a mantle heater to decompose organic matter. After pyrolysis, the residue carbon species was removed completely by heating at 823 K for 2 h using a box furnace. The oxide precursors thus obtained were amorphous. Nitridation of the oxide precursors was performed at 1073–1273 K for 10 h in a stream of pure NH_3 , 5% NH_3-N_2 , or moist- NH_3 with a flow rate of 100 mL min^{-1} using a tubular furnace. The moist- NH_3 flow was achieved by bubbling NH_3 gas through a saturated aqueous ammonia solution at 298 K.

2.2. Characterization of $Ba_{3-x}La_xTa_5O_{14-x}N_{1+x}$

Crystal phases of samples were identified by powder X-ray diffraction technique with $Cu K\alpha$ radiation (XRD; Bruker AXS, D2 Phaser). Diffuse reflectance spectra in ultraviolet-visible region (UV-vis) were taken by an absorption spectrometer (Shimadzu, UV-3100) using an integrating sphere. Contents of N were analyzed by a combustion analyzer (Horiba, EMGA-620W). The composition at surface was determined by X-ray photoelectron spectroscopy (XPS; Kratos, ESCA-3200). The samples were observed by a scanning electron microscope (SEM; Hitachi, SU1510). Specific surface areas of the samples were determined by the BET method from N_2 adsorption isotherms (Micromeritics, ASAP-2010).

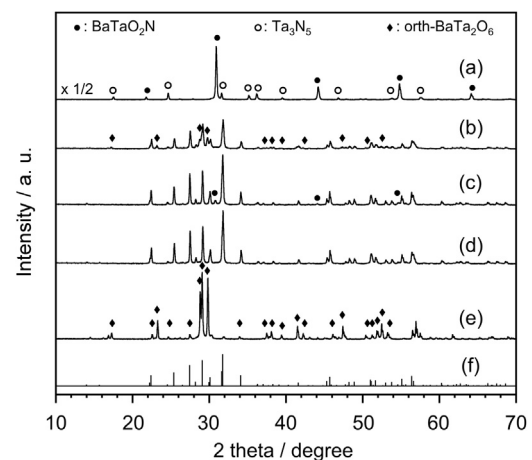


Fig. 2. XRD patterns of the samples obtained by nitridation of oxide precursors with $Ba:Ta = (a-d) 3:5$ and (e) 1:2 under various conditions; (a) 100% NH_3 , 1273 K, (b) 5% NH_3-N_2 , 1073 K, (c) 5% NH_3 , 1173 K, (d, e) moist- NH_3 , 1273 K. A simulated pattern of $Ba_3Ta_5O_{14}N$ is also presented as (f).

2.3. Evaluation of photocatalytic properties

Photocatalytic activities for H_2 and O_2 evolution in the presence of sacrificial reagents were measured using a gas-closed circulation system. The samples modified with 0.3 wt% of a Pt cocatalyst were used for H_2 evolution tests. Reactant solutions were 20 vol% methanol/water solution for H_2 evolution and 20 mM aqueous $AgNO_3$ solution with 0.1 g of La_2O_3 powder as a pH buffer reagent for O_2 evolution. Photocatalyst (0.1 g) was dispersed in 150 mL of reactant solution in a reaction vessel with a top-window. Ten kPa of Ar was introduced into the system after deaeration. The suspended solution was irradiated with visible light ($\lambda > 420\text{ nm}$) using a 300 W Xe-arc lamp (Excelitas, Cermax PE300BF) with an optical cut-off filter. Monochromatic light from an illumination system (Asahi Spectra, MAX-303) was used for analysis of action spectra. Evolved gas was analyzed using an online gas chromatograph (Shimadzu, GC-14 B with MS-5A column, TCD detector, and Ar carrier). Apparent quantum efficiencies (η_{app}) were determined by following equation,

$$\eta_{app}(\%) = (R_{H_2} \times 2) / \{I / ((1240/\lambda) \times 1.602 \times 10^{19} \times N_A)\} \times 100$$

where R_{H_2} , I , λ and N_A represent the rate of H_2 production in a unit of mol s^{-1} , power of the monochromatic incident light in a unit of J s^{-1} (W), wavelength of monochromatic light in a nm unit and the Avogadro constant, respectively.

3. Results and discussion

3.1. Synthesis condition of $Ba_3Ta_5O_{14}N$

Nitridation of the oxide precursor with $Ba:Ta = 3:5$ was conducted under various conditions to find suitable nitridation condition for $Ba_3Ta_5O_{14}N$ (Fig. 2). The sample nitridized under pure NH_3 contained no TTB phases and was a mixture of perovskite-type $BaTaO_2N$ and Ta_3N_5 . This result suggested that nitridation reaction proceeded too much for $Ba_3Ta_5O_{14}N$ under pure NH_3 . Then, nitridation using 5% NH_3-N_2 was conducted to reduce the degree of nitridation. The TTB compound was formed as a major phase with small amount of $BaTaO_2N$ impurity in nitridation at 1173 K whereas a mixture of TTB compound and orth-BaTa₂O₆ was obtained by nitridation at 1073 K. When nitridation was performed under a moist- NH_3 flow, single phase of TTB compound was obtained. The samples obtained by nitridation using 5% NH_3-N_2 or moist- NH_3 were basically pale yellow although the sample nitridized at 1173 K

under 5% $\text{NH}_3\text{-N}_2$ was reddish pale yellow due to the presence of trace amount of red BaTaO_2N . The results indicate that the TTB compound formed by the nitridation was TTB oxynitride $\text{Ba}_3\text{Ta}_5\text{O}_{14}\text{N}$ rather than tetr- BaTa_2O_6 that is one kind of the TTB oxides. In addition, when an oxide precursor with a ratio of $\text{Ba:Ta} = 2.5:5$ corresponding to the oxide phase BaTa_2O_6 was treated at 1273 K under the moist- NH_3 flow, orth- BaTa_2O_6 of the low temperature polymorph of BaTa_2O_6 was obtained as a main phase. Thus, being the ratio of $\text{Ba:Ta} = 3:5$ is essential to obtain pale yellow TTB compound by nitridation of Ba-Ta oxide. These results clearly indicate that the TTB compound formed by nitridation of precursor with $\text{Ba:Ta} = 3:5$ is not nitrogen-doped tetr- $\text{BaTa}_2\text{O}_{6-3x}\text{N}_{2x}$ but $\text{Ba}_3\text{Ta}_5\text{O}_{14}\text{N}$. Indeed, the analyzed content of nitrogen was of 0.85 wt% in the single phase of TTB compound (moist- NH_3 sample) and was well consistent with the ideal value of $\text{Ba}_3\text{Ta}_5\text{O}_{14}\text{N}$ (0.90 wt%). Thus, the present research reveals that synthesis of $\text{Ba}_3\text{Ta}_5\text{O}_{14}\text{N}$ in high phase purity is possible by nitridation of the oxide precursor using 5% $\text{NH}_3\text{-N}_2$ or moist NH_3 flow beside $\text{NH}_3\text{-O}_2$ flow reported previously [22].

3.2. Synthesis and characterization of $\text{Ba}_{3-x}\text{La}_x\text{Ta}_5\text{O}_{14-x}\text{N}_{1+x}$

We have previously reported that the increase in nitrogen content narrows band gaps of perovskite-type oxynitrides [21]. Substitution of La^{3+} for Ba^{2+} is possible strategy to increase the nitrogen content of TTB-type oxynitride according to formula $\text{Ba}_{3-x}\text{La}_x\text{Ta}_5\text{O}_{14-x}\text{N}_{1+x}$. Fig. 3A shows XRD patterns of the samples obtained by nitridation of oxide precursors with $\text{Ba:La:Ta} = 3-x:x:5$ under the moist- NH_3 flow at 1273 K. The samples with $x = 0.5$ and 1.0 were obtained as a single phase of the TTB compound as well as $\text{Ba}_3\text{Ta}_5\text{O}_{14}\text{N}$ ($x = 0$) while the $x = 1.5$ sample was a mixture of TTB compound, Ta_3N_5 , and LaTaO_4 . Thus, the phase pure TTB oxynitride was obtained in cases with $x \leq 1$. This limit is owing to characteristics of the TTB structure. Two kinds of A-sites, that are 12-fold coordination site for A1 and 15-fold one for A2, exist in the TTB structure ((A1)(A2)₂ B_5X_{15}) as shown in Fig. 1. Although there are many TTB compounds in $\text{K}_2\text{LnTa}_5\text{O}_{15}$, $\text{KAE}_2\text{Ta}_5\text{O}_{15}$ ($\text{AE} = \text{Sr}$ and Ba), and $\text{NaAE}_2\text{Ta}_5\text{O}_{15}$ systems, TTB compounds possessing smaller A-site cations than Sr^{2+} exceeding 1/3 of total A-sites, such as $\text{Na}_2\text{LnTa}_5\text{O}_{15}$, $\text{KCa}_2\text{Ta}_5\text{O}_{15}$ and $\text{NaCaSrTa}_5\text{O}_{15}$, have never been reported. It is because that only large cations such as Sr^{2+} , Ba^{2+} , and K^+ can occupy the A2-sites. According to this rule, A2-sites should be occupied by Ba^{2+} in the case of $\text{Ba}_{3-x}\text{La}_x\text{Ta}_5\text{O}_{14-x}\text{N}_{1+x}$, meaning that the limit of lanthanum substitution is $x = 1$. The contents of nitrogen in the samples increased with the La-substitution and were in good agreement with ideal values as shown in Table 1.

The synthesis of $\text{Ba}_{3-x}\text{La}_x\text{Ta}_5\text{O}_{14-x}\text{N}_{1+x}$ was attempted using 5% $\text{NH}_3\text{-N}_2$ (Fig. 3B). Phase pure TTB compounds were obtained for $x = 0.5$ and 1.0 as well as synthesis using moist- NH_3 although

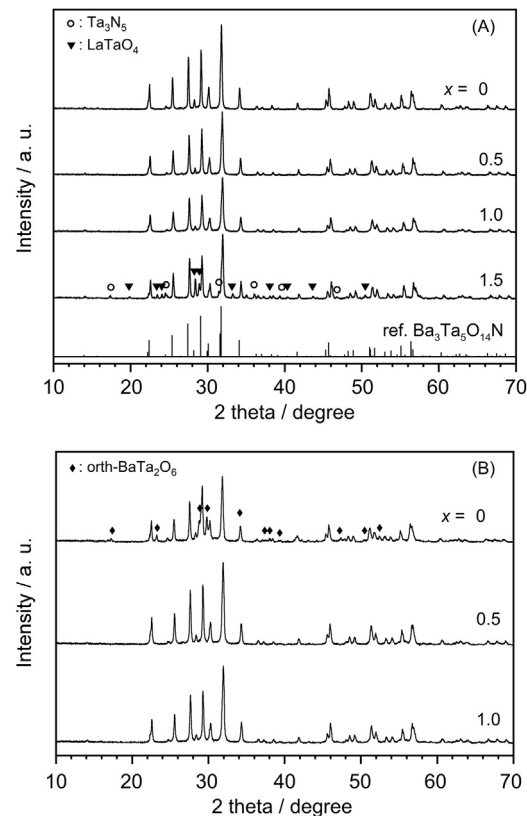


Fig. 3. XRD patterns of $\text{Ba}_{3-x}\text{La}_x\text{Ta}_5\text{O}_{14-x}\text{N}_{1+x}$ obtained by nitridation using (A) moist- NH_3 at 1273 K for 10 h and (B) 5% NH_3 at 1073 K for 10 h.

$\text{Ba}_3\text{Ta}_5\text{O}_{14}\text{N}$ was not obtained as a single phase as described above. Thus, the window of synthesis conditions especially of nitriding atmosphere is expanded by the La-substitution. The increase in the target content of nitrogen by La-substitution would improve easiness in the synthesis of TTB-type oxynitride. The sharpness, intensity, and position of diffraction peaks were almost the same between samples synthesized in moist- NH_3 and 5% NH_3 (Fig. S1). Moreover, no remarkable differences in contents of nitrogen were seen between samples synthesized under moist- NH_3 and 5% NH_3 . Thus, both samples were identical with respect to bulk properties.

Fig. 4 shows UV-vis spectra of the samples obtained as phase pure TTB compounds. An absorption edge of $\text{Ba}_3\text{Ta}_5\text{O}_{14}$ remarkably shifted in comparison with that of tetr- BaTa_2O_6 which is an A-site deficient TTB oxide. The band gap of $\text{Ba}_3\text{Ta}_5\text{O}_{14}$ is estimated to be 2.8 eV, which consists with the value in the previous report [22]. The

Table 1
Photocatalytic activity of $\text{Ba}_{3-x}\text{La}_x\text{Ta}_5\text{O}_{14-x}\text{N}_{1+x}$ under visible light.

x	Synthesis condition	N content ^a / wt%	N/Ta ratio ^b	Activity / $\mu\text{mol h}^{-1}$	
				H_2^{c}	O_2^{d}
0	Moist- NH_3	0.85/0.90	0.07	0.8	0.3
	Annealed/moist- NH_3	1.00/0.90	0.21	1.9	0.9
0.5	Moist- NH_3	1.17/1.35	ND ^e	0.8	0.4
	5% $\text{NH}_3\text{-N}_2$	1.18/1.35	ND ^e	1.5	0.3
1	Moist- NH_3	1.58/1.80	0.14	0.7	0.3
	Annealed/moist- NH_3	2.05/1.80	0.33	2.6	0.3
	5% $\text{NH}_3\text{-N}_2$	1.63/1.80	0.22	3.7	0.3

^a Measured value/identical value.

^b Determined from XPS analysis.

^c Measured for Pt (0.3 wt%)-loaded sample.

^d Measured without cocatalyst.

^e Not determined.

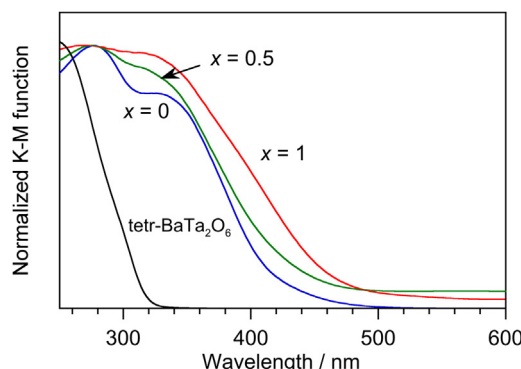


Fig. 4. UV-vis spectra of $\text{Ba}_{3-x}\text{L}_{\text{a}}\text{x}\text{Ta}_5\text{O}_{14-x}\text{N}_{1+x}$.

remarkable red shift is due to contribution of N 2p orbital to band structure. In the absorption spectrum of $\text{Ba}_3\text{Ta}_5\text{O}_{14}$, an absorption band appears in UV region. This absorption band is similar to band gap absorption in tetr-BaTa₂O₆ corresponding to electron transition from O 2p to Ta 5d. This result suggests that N 2p orbitals form electron donor levels rather than valence band. It is reasonable in consideration of small contribution of N 2p owing to low concentration of N in $\text{Ba}_3\text{Ta}_5\text{O}_{14}\text{N}$. The absorption in visible region became intense as increasing La-substitution and the absorption band owing to transition from O 2p to Ta 5d became unobvious. Thus, enhancement of visible light absorption is achieved by increasing the content of nitrogen with La-substitution.

3.3. Photocatalytic activity of $\text{Ba}_{3-x}\text{L}_{\text{a}}\text{x}\text{Ta}_5\text{O}_{14-x}\text{N}_{1+x}$

Photocatalytic activities of $\text{Ba}_{3-x}\text{L}_{\text{a}}\text{x}\text{Ta}_5\text{O}_{14-x}\text{N}_{1+x}$ are summarized in Table 1. All samples exhibited photocatalytic H₂ and O₂ evolution in the presence of sacrificial reagents under visible light. The samples synthesized under moist-NH₃ evolved H₂ in rates of 0.7–0.8 $\mu\text{mol}/\text{h}$ irrespective of the composition. The samples synthesized in 5% NH₃ showed higher activity for H₂ evolution than ones synthesized moist-NH₃. The activity of $\text{Ba}_2\text{LaTa}_5\text{O}_{13}\text{N}_2$ for H₂ evolution was higher than that of $\text{Ba}_{2.5}\text{La}_{0.5}\text{Ta}_5\text{O}_{13.5}\text{N}_{1.5}$. As mentioned above, there are no differences in crystallinity and contents of nitrogen between samples synthesized in moist-NH₃ and 5% NH₃. Moreover, there are no differences in morphological properties between the moist-NH₃ and 5% NH₃ samples of $\text{Ba}_2\text{LaTa}_5\text{O}_{13}\text{N}_2$, that is, both samples are composed of large secondary particles in which fine featureless primary particles are aggregated and sintered as shown in Fig. S2. However, XPS analysis of $\text{Ba}_2\text{LaTa}_5\text{O}_{13}\text{N}_2$ revealed that the ratio of nitrogen at the surface changed by the nitriding atmosphere although no change in chemical states of Ta and N (Fig. 5a and c). The ratio of N/Ta was 0.14 in the moist-NH₃ sample while that was increased to 0.22 in the 5% NH₃ sample (Table 1). Partial oxidation of surface by water vapor competitively occurs in nitridation process using moist-NH₃ [48], resulting in the poor nitrogen surface. These results suggest that the low activities of the moist-NH₃ samples are due to the nitrogen poor surfaces (Fig. 6). Annealing treatment at 1073 K for 10 h using 5% NH₃ was performed for the moist-NH₃ samples of $\text{Ba}_3\text{Ta}_5\text{O}_{14}\text{N}$ and $\text{Ba}_2\text{LaTa}_5\text{O}_{13}\text{N}_2$ to modify the surfaces. No changes in chemical states of Ta and N were observed again in XPS analysis (Fig. 5a and b). However, the ratio of N/Ta in XPS analysis greatly increased from 0.14 to 0.33 by the annealing treatment of $\text{Ba}_2\text{LaTa}_5\text{O}_{13}\text{N}_2$ whereas the slight increase in the bulk content of nitrogen and no changes in XRD patterns were observed as shown in Table 1 and Fig. S3. The similar effects of the annealing treatment were also observed for $\text{Ba}_3\text{Ta}_5\text{O}_{14}\text{N}$ without morphological changes (Fig. S4). Thus, annealing treatment using 5% NH₃ at 1073 K mainly affected the

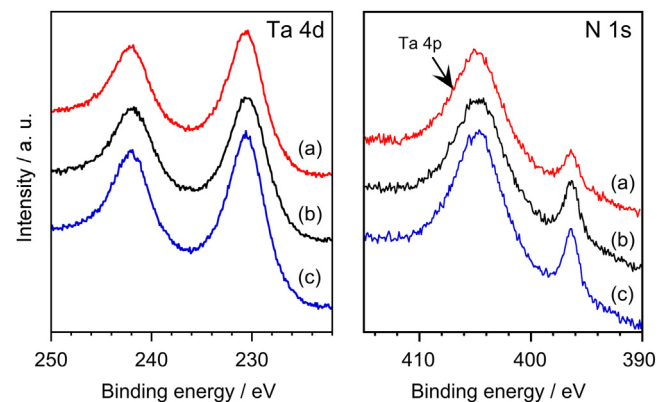


Fig. 5. XPS in Ta 4d and N 1s regions of $\text{Ba}_2\text{LaTa}_5\text{O}_{13}\text{N}_2$: (a) synthesized in moist-NH₃, (b) annealed (a), and (c) synthesized in 5% NH₃.

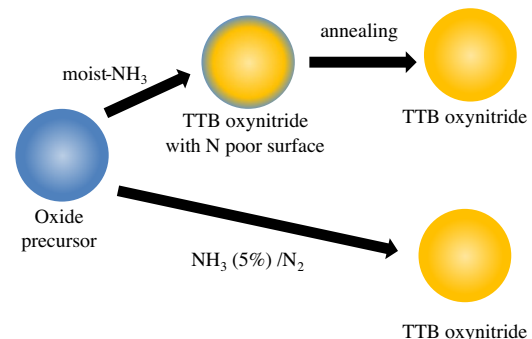


Fig. 6. Changes in surface status by synthesis methods.

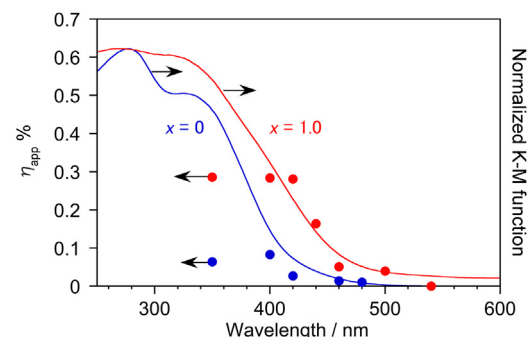


Fig. 7. Action spectra of $\text{Ba}_3\text{Ta}_5\text{O}_{14}\text{N}$ and $\text{Ba}_2\text{LaTa}_5\text{O}_{13}\text{N}_2$ ($x=1$) for H₂ evolution together with their UV-vis spectra.

surface properties. The activities of both samples for H₂ evolution were improved by the annealing treatment. However, for O₂ evolution, annealing treatment improved the activity of $\text{Ba}_3\text{Ta}_5\text{O}_{14}\text{N}$ but did not affect for $\text{Ba}_2\text{LaTa}_5\text{O}_{13}\text{N}_2$. The specific surface area of $\text{Ba}_2\text{LaTa}_5\text{O}_{13}\text{N}_2$ ($6.5 \text{ m}^2 \text{ g}^{-1}$) was larger than that of $\text{Ba}_3\text{Ta}_5\text{O}_{14}\text{N}$ ($2.5 \text{ m}^2 \text{ g}^{-1}$), indicating $\text{Ba}_2\text{LaTa}_5\text{O}_{13}\text{N}_2$ composed of smaller particles. It has been reported that small particles are not effective for photocatalytic O₂ evolution of a 4-electron reaction [49]. It is assumed that O₂ evolution is tough for $\text{Ba}_2\text{LaTa}_5\text{O}_{13}\text{N}_2$ composed of small particles, resulting in a poor effect of the annealing treatment.

Action spectra of $\text{Ba}_3\text{Ta}_5\text{O}_{14}\text{N}$ and $\text{Ba}_2\text{LaTa}_5\text{O}_{13}\text{N}_2$ for H₂ evolution are shown in Fig. 7 together with their UV-vis spectra. The annealed moist-NH₃ sample and the 5% NH₃ sample were used for $\text{Ba}_3\text{Ta}_5\text{O}_{14}\text{N}$ and $\text{Ba}_2\text{LaTa}_5\text{O}_{13}\text{N}_2$, respectively, in measurement of action spectra. $\text{Ba}_2\text{LaTa}_5\text{O}_{13}\text{N}_2$ showed higher η_{app} than $\text{Ba}_3\text{Ta}_5\text{O}_{14}\text{N}$ in entire range; for example 0.3% and 0.1% at 400 nm. The larger mobility of photogenerated holes, which is

caused by the larger contribution of N 2p orbital owing to higher content of nitrogen in $\text{Ba}_2\text{LaTa}_5\text{O}_{13}\text{N}_2$, would result in higher η_{app} . In addition, an onset wavelength in the action spectrum of $\text{Ba}_2\text{LaTa}_5\text{O}_{13}\text{N}_2$ was obviously shifted to longer wavelength side like as UV-vis spectrum. However, η_{app} at 350 nm was almost the same as that at 400 nm although larger numbers of photogenerated e^-/h^+ pairs were expected from stronger absorption at 350 nm. The factors other than surface reactivity and photogeneration of e^-/h^+ would limit η_{app} . The interior and/or inter-particle mobility of e^-/h^+ would be still low although the mobility of holes is improved by increasing the nitrogen content. Such low mobility of photogenerated carriers spoil the advantage of larger number of photogenerated e^-/h^+ , resulting in the relatively low apparent quantum efficiencies at 350 nm. As described above, it has found that La-substitution improves photocatalytic activity of TTB oxynitride with points of view not only from the increase in the ability of visible light absorption but also from enhancement of efficiency.

4. Conclusions

TTB oxynitrides $\text{Ba}_{3-x}\text{La}_x\text{Ta}_5\text{O}_{14-x}\text{N}_{1+x}$ ($x=0$, 0.5, and 1) have been successfully synthesized using moist- NH_3 as a nitriding atmosphere whereas TTB oxynitride with $x > 1.5$ has not be obtained. It is concluded that the limit of La-substitution is $x = 1$ because small cation La^{3+} cannot occupy the 15-fold site. TTB oxynitrides with $x=0.5$ and 1 can also be obtained in pure phase using 5% NH_3 as a nitriding atmosphere. TTB oxynitrides exhibit photocatalytic activities for sacrificial H_2 and O_2 evolution under visible light. The samples synthesized under moist- NH_3 show lower activities than the samples synthesized or annealed in 5% NH_3 atmosphere. Low activities of the moist- NH_3 sample are due to the nitrogen poor surfaces. Thus, it has been found that the annealing treatment using diluted NH_3 gas is one of the ways to improve the photocatalytic activity of oxynitrides. The increase in the content of nitrogen achieved by the La-substitution causes red-shifts of onset wavelengths in absorption and action spectra. It is presumed that the larger contribution of N 2p orbital also enhances photocatalytic efficiency of TTB oxynitrides due to the improvement of the mobility of photogenerated holes.

Acknowledgements

This work was partly supported by KAKENHI Grant Numbers JP24107004 from MEXT and JP16H04186 from JSPS, Japan. The authors thank Prof. M. Hara at Tokyo Institute of Technology for his help for XPS measurement.

Appendix A. Supplementary data

Supplementary data associated with this article can be found, in the online version, at <http://dx.doi.org/10.1016/j.apcatb.2017.01.057>.

References

- [1] F.E. Oserloh, Chem. Mater. 20 (2008) 35–54.
- [2] A. Kudo, Y. Miseki, Chem. Soc. Rev. 38 (2009) 253–278.
- [3] X. Chen, S. Shen, L. Guo, S. Mao, Chem. Rev. 110 (2010) 6503–6570.
- [4] K. Maeda, K. Domen, J. Phys. Chem. Lett. 1 (2010) 2655–2661.
- [5] B.A. Pinaud, J.D. Benck, L.C. Seitz, A.J. Forman, Z. Chen, T.G. Deutsch, B.D. James, K.N. Baum, G.N. Baum, S. Ardo, H. Wang, E. Miller, T.F. Jaramillo, Energy Environ. Sci. 6 (2013) 1983–2002.
- [6] X. Wang, K. Maeda, A. Thomas, K. Takanabe, G. Xin, J.M. Carlsson, K. Domen, M. Antonietti, Nat. Mater. 8 (2009) 76–80.
- [7] M. Tabata, K. Maeda, T. Ishihara, T. Minegishi, T. Takata, K. Domen, J. Phys. Chem. C 114 (2010) 11215–11220.
- [8] Q. Jia, Y. Miseki, K. Saito, H. Kobayashi, A. Kudo, Bull. Chem. Soc. Jpn. 83 (2010) 1275–1281.
- [9] Z. Yi, J. Ye, N. Kikugawa, T. Kako, S. Ouyang, H. Stuart-Williams, H. Yang, J. Cao, W. Luo, Z. Li, Y. Liu, R.L. Withers, Nat. Mater. 9 (2010) 559–564.
- [10] J.S. Jang, P.H. Borse, J.S. Lee, K.T. Lim, C.R. Cho, E.D. Jeong, M.G. Ha, M.S. Won, H.G. Kim, J. NanoScale Nanotechnol. 10 (2010) 5008–5014.
- [11] Y. Miseki, A. Kudo, ChemSusChem 4 (2011) 245–251.
- [12] S. Chen, J. Yang, C. Ding, R. Li, S. Jin, D. Wang, H. Han, F. Zhang, C. Li, J. Mater. Chem. A 1 (2013) 5651–5659.
- [13] T. Hisatomi, C. Katayama, Y. Moriya, T. Minegishi, M. Katayama, H. Nishiyama, T. Yamada, K. Domen, Energy Environ. Sci. 6 (2013) 3595–3599.
- [14] P.P. Sahoo, P.A. Maggard, Inorg. Chem. 52 (2013) 4443–4450.
- [15] H. Kato, A. Takeda, M. Kobayashi, M. Kakihana, Chem. Lett. 42 (2013) 744–746.
- [16] H. Kato, A. Takeda, M. Kobayashi, M. Hara, M. Kakihana, Catal. Sci. Technol. 3 (2013) 3147–3154.
- [17] K. Maeda, K. Domen, Bull. Chem. Soc. Jpn. 89 (2013) 627–648.
- [18] L. Wang, B. Cao, W. Kang, M. Hybertsen, K. Maeda, K. Domen, P.G. Khalifah, Inorg. Chem. 52 (2013) 9192–9205.
- [19] S. Chen, Y. Qi, T. Hisatomi, Q. Ding, T. Asai, Z. Li, S.S. Ma, F. Zhang, K. Domen, C. Li, Angew. Chem. Int. Ed. 54 (2015) 8498–8501.
- [20] H. Kato, T. Fujisawa, M. Kobayashi, M. Kakihana, Chem. Lett. 44 (2015) 973–975.
- [21] H. Kato, K. Ueda, M. Kobayashi, M. Kakihana, J. Mater. Chem. A 3 (2015) 11824–11829.
- [22] B. Anke, T. Bredow, J. Soldat, M. Wark, M. Lerch, J. Solid State Chem. 233 (2016) 282–288.
- [23] H. Fujito, H. Kunioku, D. Kato, H. Suzuki, M. Higashi, H. Kageyama, R. Abe, J. Am. Chem. Soc. 138 (2016) 2082–2085.
- [24] K. Domen, S. Naito, M. Soma, T. Onishi, K. Tamaru, J. Chem. Soc. Chem. Commun. (1980) 543–544.
- [25] K. Maeda, K. Teramura, D. Lu, N. Saito, Y. Inoue, K. Domen, Angew. Chem. Int. Ed. 45 (2006) 7806–7809.
- [26] K. Maeda, K. Teramura, N. Saito, Y. Inoue, K. Domen, J. Catal. 243 (2006) 303–308.
- [27] A. Iwase, H. Kato, A. Kudo, Catal. Lett. 108 (2006) 7–10.
- [28] J.J.H. Pijpers, M.T. Winkler, Y. Surendranath, T. Buonassisi, D.G. Nocera, Proc. Natl. Acad. Sci. U. S. A. 108 (2011) 10056–10061.
- [29] J. Yang, D. Wang, H. Han, C. Li, Acc. Chem. Res. 46 (2013) 1900–1909.
- [30] T. Kanazawa, D. Lu, K. Maeda, Chem. Lett. 45 (2016) 967–969.
- [31] A.E. Maegli, T. Hisatomi, E.H. Otal, S. Yoon, S. Pokrant, M. Grätzel, A. Weidenkaff, J. Mater. Chem. 22 (2012) 17906–17913.
- [32] H. Kato, Y. Sasaki, N. Shirakura, A. Kudo, J. Mater. Chem. A 1 (2013) 12327–12333.
- [33] H. Kato, M. Kobayashi, M. Hara, M. Kakihana, Catal. Sci. Technol. 3 (2013) 1733–1738.
- [34] Y. Mizuno, H. Wagata, K. Yubuta, N. Zettsu, S. Oishi, K. Teshima, CrystEngComm 15 (2013) 8133–8138.
- [35] D. Noureldine, D.H. Anjum, K. Takanabe, Phys. Chem. Chem. Phys. 16 (2014) 10762–10769.
- [36] T. Hisatomi, C. Katayama, K. Teramura, T. Takata, Y. Moriya, T. Minegishi, M. Katayama, H. Nishiyama, T. Yamada, K. Domen, ChemSusChem 7 (2014) 2016–2021.
- [37] T. Takayama, A. Iwase, A. Kudo, Bull. Chem. Soc. Jpn. 88 (2015) 538–543.
- [38] C.S. Quintans, H. Kato, M. Kobayashi, H. Kaga, A. Iwase, A. Kudo, M. Kakihana, J. Mater. Chem. A 3 (2015) 14239–14244.
- [39] A. Iwase, Y.H. Ng, Y. Ishiguro, A. Kudo, R. Amal, J. Am. Chem. Soc. 133 (2011) 11054–11057.
- [40] M. Matsukawa, R. Ishikawa, T. Hisatomi, Y. Moriya, N. Shibata, J. Kubota, Y. Ikuhara, K. Domen, Nano Lett. 14 (2014) 1038–1041.
- [41] C. Pan, T. Takata, M. Nakabayashi, T. Matsumoto, N. Shibata, Y. Ikuhara, K. Domen, Angew. Chem. Int. Ed. 54 (2015) 295–2959.
- [42] T. Takata, C. Pan, M. Nakabayashi, N. Shibata, K. Domen, J. Am. Chem. Soc. 137 (2015) 9627–9634.
- [43] Q. Wang, T. Hisatomi, Q. Jia, H. Tokudome, M. Zhong, C. Wang, Z. Pan, T. Takata, M. Nakabayashi, N. Shibata, Y. Li, I.D. Sharp, A. Kudo, T. Yamada, K. Domen, Nat. Mater. 15 (2016) 611–615.
- [44] H. Kato, K. Asakura, A. Kudo, J. Am. Chem. Soc. 125 (2003) 3082–3089.
- [45] Y. Ham, T. Hisatomi, Y. Goto, Y. Moriya, Y. Sakata, A. Yamakata, J. Kubota, K. Domen, J. Mater. Chem. A 4 (2016) 3027–3033.
- [46] R. Konta, T. Ishii, H. Kato, A. Kudo, J. Phys. Chem. B 108 (2004) 8992–8995.
- [47] K. Maeda, K. Domen, J. Phys. Chem. C 111 (2007) 7851–7861.
- [48] E. Orhan, F. Tessier, R. Marchand, Solid State Sci. 4 (2002) 1071–1076.
- [49] F. Amano, E. Ishinaga, A. Yamakata, J. Phys. Chem. C 117 (2013) 22584–22590.